Pergamon

Cement and Concrete Research 30 (2000) 457–464

CEMENT AND CONCRETE RESEARCH

Microstructural investigations on aerated concrete

N. Narayanan, K. Ramamurthy*

Building Technology and Construction Management Division, Department of Civil Engineering, Indian Institute of Technology Madras, Chennai 600 036, India

Received 13 June 1999; accepted 27 December 1999

Abstract

Aerated concrete is characterized by the presence of large voids deliberately included in its matrix to reduce the density. This study reports the investigations conducted on the structure of cement-based autoclaved aerated concrete (AAC) and non-AAC with sand or fly ash as the filler. The reasons for changes in compressive strength and drying shrinkage are explained with reference to the changes in the microstructure. Compositional analysis was carried out using XRD. It was observed that fly ash responds poorly to autoclaving. The process of pore refinement in fly ash mixes is discussed with reference to the formation of Hadley grains as well as fly ash hydration. The paste–void interface in aerated concrete investigated in relation to the paste–aggregate interface in normal concrete revealed the existence of an interfacial transition zone.

Keywords: Aerated concrete; Fly ash; SEM; Microstructure; Interfacial transition zone

1. Introduction

Aerated concrete is basically a mortar, with pulverized sand and/or industrial waste like fly ash as filler, in which air is entrapped artificially by chemical (metallic powders like Al, Zn, H_2O_2) or mechanical (foaming agents) means, resulting in significant reduction in density. The composition and method of curing influence the microstructure and thus the physical and mechanical properties of aerated concrete.

Available literature classifies the porous system of autoclaved aerated concrete (AAC) with the objective of studying the water transport phenomena as: (i) artificial air pores, inter-cluster pores, and inter-particle pores [1]; (ii) macropores formed due to the expansion of the mass caused by aeration, and micropores which appear in the walls between the macropores [2]; and (iii) microcapillaries (<50 nm) and macrocapillaries (50 nm to 50 μm) [3]. Since the air void system is stated to remain largely identical for moist-cured and AAC [4], the variation in its properties due to changes in composition and curing methods can only be explained by a study on the microstructure of hydration products and the void–paste interface. Hence, a study on the microstructural characteristics of aerated concrete has been undertaken and the results are discussed in this article in terms of (i) structure of the products of hydration, (ii) pore refinement due to addition of fly ash, and (iii) interfacial transition zone between void and matrix.

2. Materials and methodology

The experimental investigation comprises of SEM and Powder XRD (using Co-Kα radiation) studies on moist-cured (90, 150, and 180 days) and AAC (8 and 10 h at a pressure of 10 kg/cm^2) with a mix 1:3 (cement:sand or fly ash). Ordinary Portland cement (28-day compressive strength of 44 MPa), lime with 75% CaO, pulverized river sand finer than 300-μm size and Class F fly ash as per ASTM C-618 [5] were used. The chemical analysis of cement and fly ash is shown in Table 1. The electron micrograph of fly ash in Fig. 1 shows that it consists of smooth spherical particles (Plerospheres). To supplement the alkali in cement for facilitating the generation of hydrogen gas, a fixed amount of lime was used (lime/cement = 0.25 by weight).

Powdered samples were used for the study of matrix microstructure and XRD, whereas for the investigations of

* Corresponding author. Tel.: +91-44-445-8309/9309; fax: +91-44-235-0509.

E-mail address: vivek@civil.iitm.ernet.in (K. Ramamurthy).

0008-8846/00/$ – see front matter
PII: S0008-8846(00)00199-X

Table 1
Physical and chemical characteristics of cement and fly ash

Properties	Cement	Fly ash
Physical		
Blaine's fineness (m^2/kg)	391	794
Specific gravity	3.12	2.20
28-day compressive strength (MPa)	44	–
Chemical		
Calcium oxide (%)	62.48	0.93
Silica (%)	20.35	56.92
Alumina (%)	5.92	33.69
Magnesia (%)	1.70	0.60
Total sulphur as SO_3 (%)	1.46	0.46
Loss on ignition (%)	2.54	1.25
Total alkali ($Na_2O + K_2O$)	1.23	–

microstructure around air voids, regular pieces of 10-mm size were cut ensuring at least one prominent artificial air pore. The specimens were kept in an oven for 24 h at 105 ± 5°C to remove evaporable water, mounted on metal stubs, and sputter-coated before subjecting to the electron beam from a JEOL 5300 Scanning Electron Microscope. Micrographs were taken at the age of 90, 150, and 180 days (after moist-curing for the first 28 days) and XRD at 90 days for moist-cured aerated concrete and immediately after curing for autoclaved specimens. As the hydration of fly ash is a relatively slow process, longer duration of moist-curing was also considered for this study.

3. Discussion of results

3.1. Microstructure of the hydration products

Compressive strengths and drying shrinkage of moist-cured and AAC with sand/fly ash for different curing conditions are presented in Table 2 and Fig. 2, respectively [6]. The salient observations pertaining to the structure and its influence on compressive strength and drying shrinkage are discussed in the following sections.

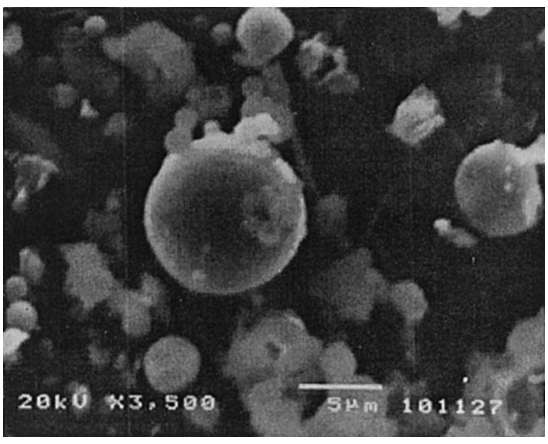

Fig. 1. Micrograph of fly ash particles showing the Plerospheres.

Table 2
Compressive strengths of moist-cured and AAC

	Compressive strength (MPa)				
	Moist-cured			Autoclaved	
Mix details	28 days	90 days	150 days	8 h	12 h
Cement–sand	7.4	7.8	7.9	12.1	14.5
Cement–fly ash	5.5	6.8	7.5	7.9	9.3

3.1.1. Moist-cured aerated concrete

Figs. 3 and 4 show the microstructure of moist-cured aerated concrete with sand and fly ash, respectively, at the age of 90 days. For aerated concrete with sand (Fig. 3), the hydration products have been more or less formed completely, indicated by the continuity in the matrix. For the products with fly ash, hydration products of cement are precipitated on the surface of some of the fly ash particles (Fig. 4) leading to encapsulation of spheres of fly ash (as fly ash is used as replacement for sand, the amount by weight is three times that of cement and hence, all fly ash particles are not encapsulated). These in turn act as nucleation sites for cement hydration [7]. Thus, the hydration is incomplete (indicated by the presence of discrete particles) and this, along with the reduced density, contributes to the lesser strength of aerated concrete with fly ash. The slow hydration of fly ash results in loss of adsorbed water from the surface of unreacted and partially reacted particles, increasing the drying shrinkage to about five times that of the product with sand (Fig. 2).

XRD pattern of aerated concrete with sand shown in Fig. 5 is characterized by the presence of C–S–H with varying C/S ratios such as C_2SH, C_2SH (B) and C_2SH (D) along with portlandite. The higher C/S ratios indicate the presence of high lime-silicate gels, which do not contribute much to strength development. Mixes with fly ash (Fig. 5) also contain these high lime-silicates in the form of C_2SH (A) and C_2SH (B) though their relative intensities are low. This apart, ettringite and hydrogarnet phases are also identified.

Micrographs of moist-cured aerated concrete with sand and fly ash, respectively, after 150 days are shown in Figs. 6 and 7. The structure of aerated concrete with sand depicted in Fig. 6 does not differ much from Fig. 3 (at 90 days) whereas for mixes with fly ash, the hydration is more complete at 150 days (Fig. 7) as compared to Fig. 4 in as much as discrete spheres are not observed. The structure at the age of 180 days in Figs. 8 and 9 show long prismatic members along with semi-crystalline gel, contrary to the structure at earlier ages (Figs. 3, 4, 6, and 7). The structure is thus unstable, changing from fibrous gel to needle to long prismatic members. Lack of interlocking among these prismatic members may be attributed as the reason for the lower strength of moist-cured aerated concrete even after complete hydration of cement.

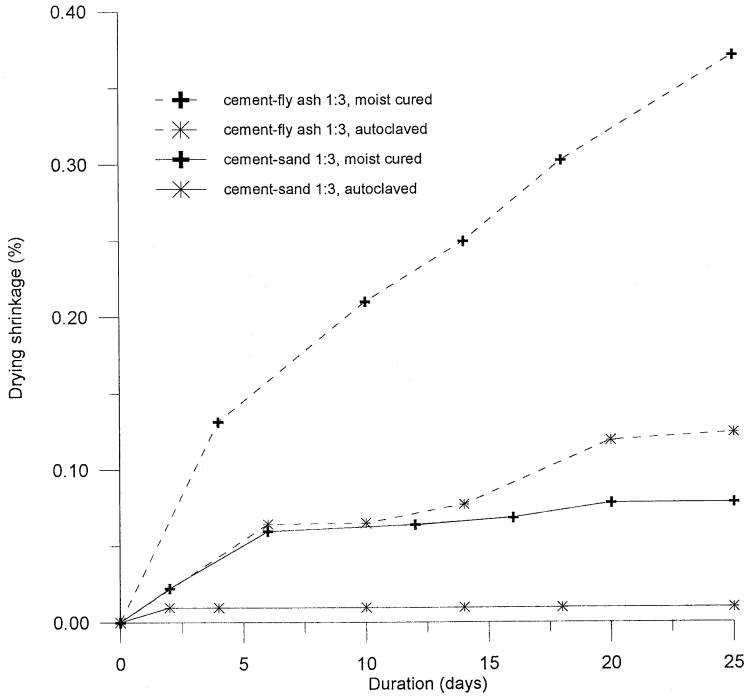

Fig. 2. Drying shrinkage of non-autoclaved and AAC.

3.1.1.1. Capillary pore refinement. The phenomena of capillary pore refinement is brought out through a discussion on (i) pozzolanic reaction of fly ash, (ii) formation and preservation of hollow shells or Hadley grains, and (iii) sorptivity studies.

Pozzolanic reaction of fly ash. A comparison of Figs. 6 and 7 (moist-cured specimen with sand and fly ash at the age of 150 days) shows that the structure is relatively homogeneous with fewer pores in the mix with fly ash than that with sand. The reason being the pozzolanic reaction between the cementitious phase of fly ash and calcium hydroxide to form C–S–H, indicating that fly ash aids in pore refinement when its reaction is almost complete. This corroborates the observations in literature on capillary pore refinement in concrete containing fly ash [7,8]. The phenomenon of capillary pore refinement is facilitated by the increase in the number of nucleation sites. The radial growth of cement hydration products on fly ash reduces the interconnectivity between the pores, resulting in a reduced capillary porosity.

Formation of hollow shell pores. Apart from the gel pores (<10 nm) and capillary pores (10 nm to 10 μm), hollow shell pores or Hadley grains have been postulated as a third type of intrinsic pore in the matrix of hydration

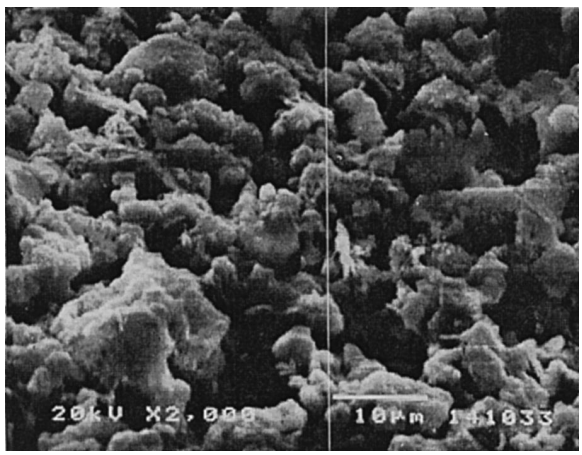

Fig. 3. Micrograph of moist-cured cement–sand aerated concrete.

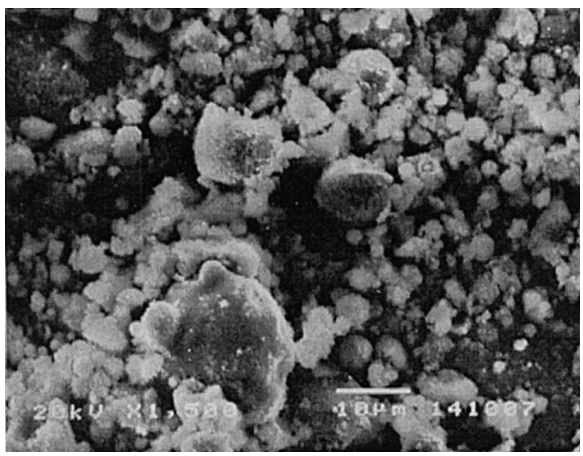

Fig. 4. Micrograph of moist-cured cement–fly ash aerated concrete (90 days).

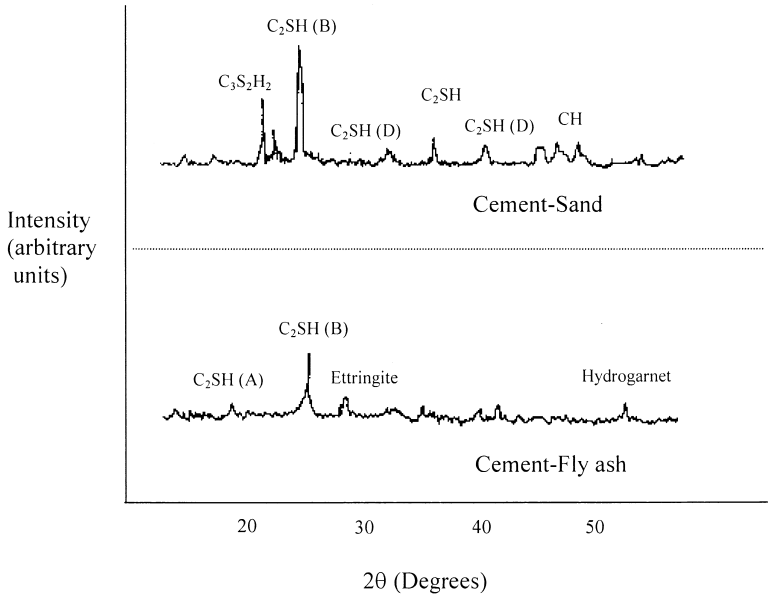

Fig. 5. XRD patterns of moist-cured aerated concrete.

products. Hollow shells are large pores (1 to around 20 μm), about the size of smaller cement grains, enclosed in cement gel and connected to the outside via capillary and gel pores. The hydration products mostly grow outwards into the capillary pore space and a void space is developed within the boundary of the original cement grains as they recede on continued hydration, forming hollow shells. Since the hydration seldom takes place within the original cement grain boundaries, the formation of hollow shells implies that the capillary pores are reduced. [9]. Hollow shell pores or Hadley grains are observed in mixes with fly ash (indicated by arrows in Fig. 7), along with densification of the capillary pore space. Since the fly ash also hydrates in the longer run, a reduced capillary porosity (pore refinement) can be considered to be a result of hollow shell hydration mechanism as well as the pozzolanic reaction. Though the pozzolanic reaction results in reduction in volume due to the loss of bound water and chemical shrinkage, it is offset by the increased volume of the hydrated products.

Sorptivity studies. Sorption characterizes the capillary absorption and transmission of water. Tests on hydraulic sorptivity of aerated concrete show (Fig. 10) that mixes with fly ash (moist-cured and autoclaved) possess lower sorptivity than the mixes with sand. This proves that fly ash contributes to the reduction of capillary pore volume.

3.1.2. Autoclaved aerated concrete

The structure of AAC with sand and fly ash (8 h of autoclaving at 10 kg/cm^2) is presented in Figs. 11 and 12. AAC with sand shows well-defined C–S–H (tobermorite) crystals and hexagonal $Ca(OH)_2$ crystals, a completely

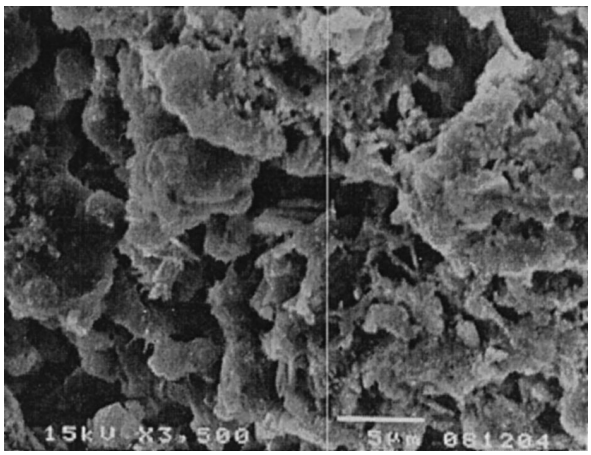

Fig. 6. Micrograph of moist-cured cement–sand aerated concrete (150 days).

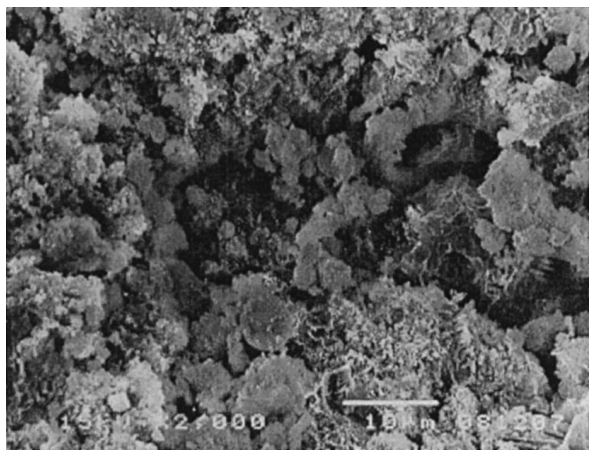

Fig. 7. Micrograph of moist-cured cement–fly ash aerated concrete (150 days).

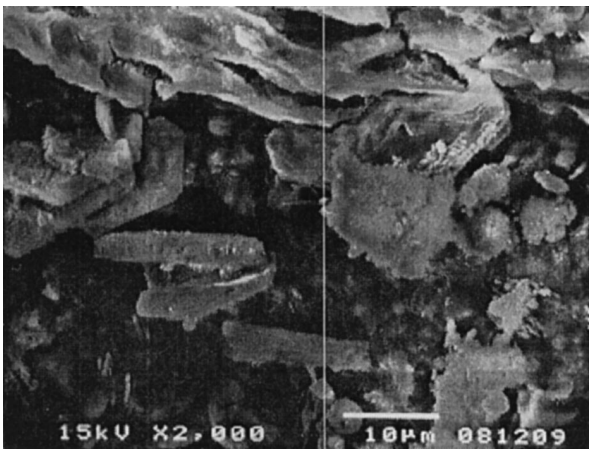

Fig. 8. Micrograph of moist-cured cement–sand aerated concrete (180 days).

different structure as compared to that of the moist-cured specimen (Fig. 3). The XRD pattern for AAC with sand shown in Fig. 13 has some high lime-silicates present in them but the presence of tobermorite underlines their crystalline structure, unlike the moist-cured one (Fig. 5). The structure of AAC with fly ash (Fig. 12) does not show complete crystallinity even though some plates of $Ca(OH)_2$ and needles of ettringite are observed. XRD of AAC with fly ash does not show as many peaks as that with sand (Fig. 13). The product is crystalline in as much as tobermorite and hydrogarnet are present, but it is the presence of the high lime-silicates with a gel-like morphology that lend these mixes a lower strength (Table 2).

When autoclaved for 12 h, the structure of AAC with fly ash also attains a crystalline nature (Fig. 14), although some unreacted particles of fly ash are observed. The crystals are broader and spaced farther apart than those formed when sand is used as filler (Fig. 11). This reduces the interlocking between the crystals and consequently, the strength. As a consequence of this microstructure, the drying shrinkage of AAC with fly ash is higher than that with sand (Fig. 2), establishing the weak influence of autoclaving on fly ash mixes.

3.2. Microstructure around air voids—interfacial transition zone

The micrograph of the pore boundary of aerated concrete shown in Fig. 15 closely resembles the model of the transition zone in normal concrete proposed by Mehta and Monteiro [10]. From this, it may be inferred that a transition zone exists in the void–paste interface of aerated concrete analogous to the one in the aggregate–paste interface of normal concrete. The larger pores in aerated concrete can be treated as aggregates of zero density and can be imagined to act as inclusions in the matrix and thereby create a *virtual* wall effect or Transition zone. The *virtual* wall is formed by a film of water in between the voids and the bulk cement paste, with the cement grains packing against this water film. Hydration compounds are formed in the outer periphery of the water film in a similar way as it is formed in the outer periphery of aggregates. This explains the similar micrographical appearance of transition zone in both normal concrete and aerated concrete.

The transition zone in normal concrete has been studied in detail by various researchers and is confirmed to be the weakest zone [11–15]; the weakness being attributed to the higher porosity at the interface as a result of the clogging of bleed water, formation of larger crystal particles of hydration, and deposition of calcium hydroxide crystals with preferential orientation. The interface in normal concrete is one between a very strong aggregate phase and a less strong matrix, whereas in lightweight aggregate concrete, the matrix is stronger than the aggregate. Since lightweight aggregates are generally porous, the cement hydration products and bleed water may permeate into the pores of the aggregate rendering the transition zone less porous than that of normal concrete [16]. In similar lines, for aerated concrete, the transition zone is between a relatively strong matrix and zero strength voids and thus will be denser and more homogeneous than the interfaces in both normal and lightweight aggregate concrete. The possible reasons for such reduction in interfacial porosity are:

1. During the process of aeration, the gas formed due to the chemical reaction (which later forms the voids) constricts the matrix;
2. The bleed water is free to move in the interface because of the absence of aggregates and the presence of large voids;
3. The absence of the aggregates allows (a) unrestricted space for hydration and growth of crystals and (b)

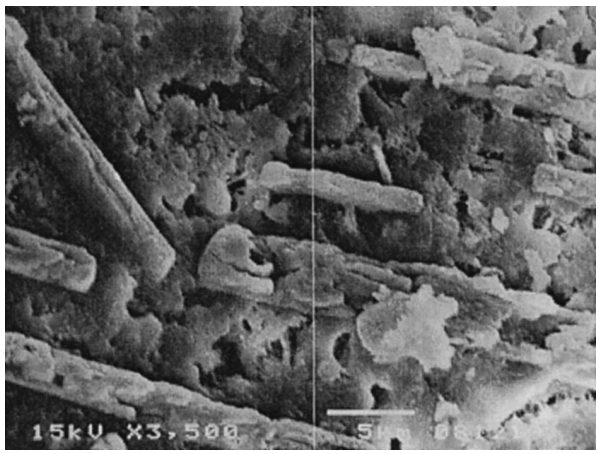

Fig. 9. Micrograph of moist-cured cement–fly ash aerated concrete (180 days).

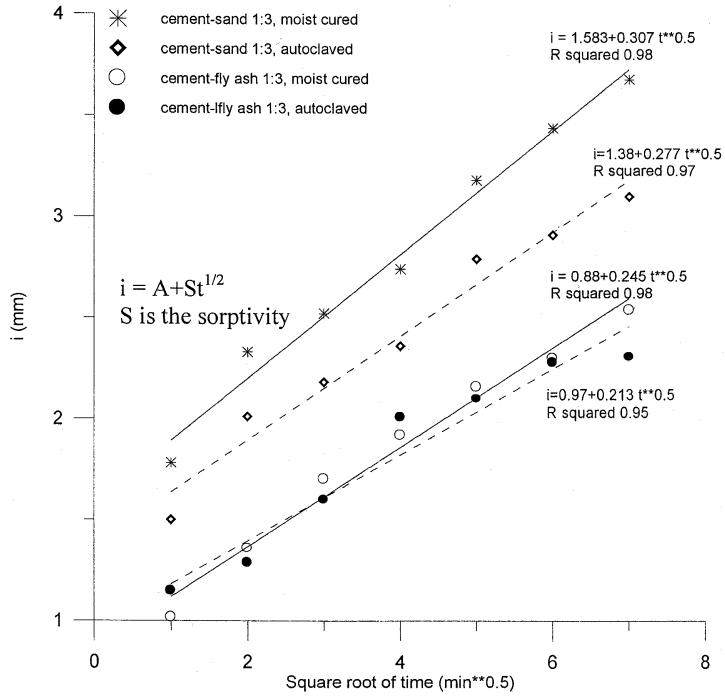

Fig. 10. Sorptivity of aerated concrete with and without fly ash.

random orientation of the crystals at the interface, resulting in better interlocking.

Also, the transition zone in aerated concrete will be denser than its bulk paste since the bulk paste essentially has pores of varying sizes. Though the structure appears similar, the transition zone in aerated concrete is likely to be significantly different from that in normal concrete as far as its influence on the properties is concerned. An in-depth characterization of this zone would be helpful in understanding the material better.

4. Conclusions

The salient conclusions as observed from the experimental investigations with reference to the composition and treatment of the samples studied are given below.

(I) The microstructural alterations, either due to compositional variation (sand/fly ash as filler) or curing (moist-curing/autoclaving) significantly affects the properties of aerated concrete.

(II) Aerated concrete with sand and fly ash as filler material exhibits considerable difference in structure be-

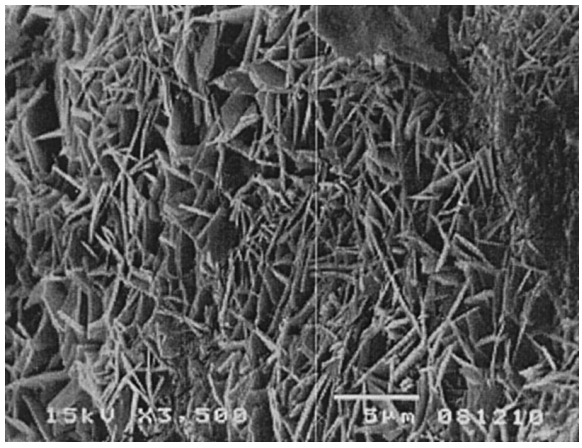

Fig. 11. Micrograph of autoclaved cement–sand aerated concrete.

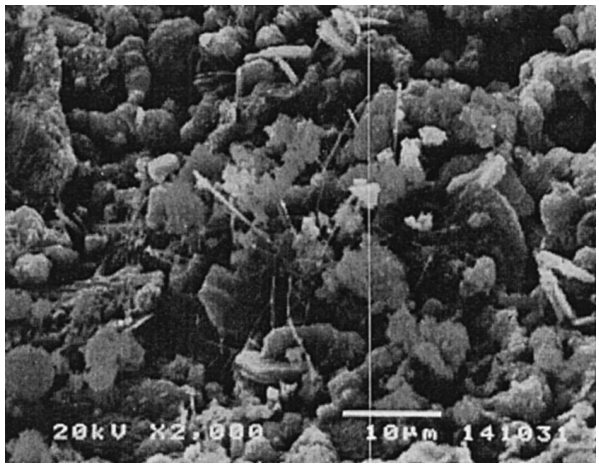

Fig. 12. Micrograph of autoclaved cement–fly ash aerated concrete (8 h).

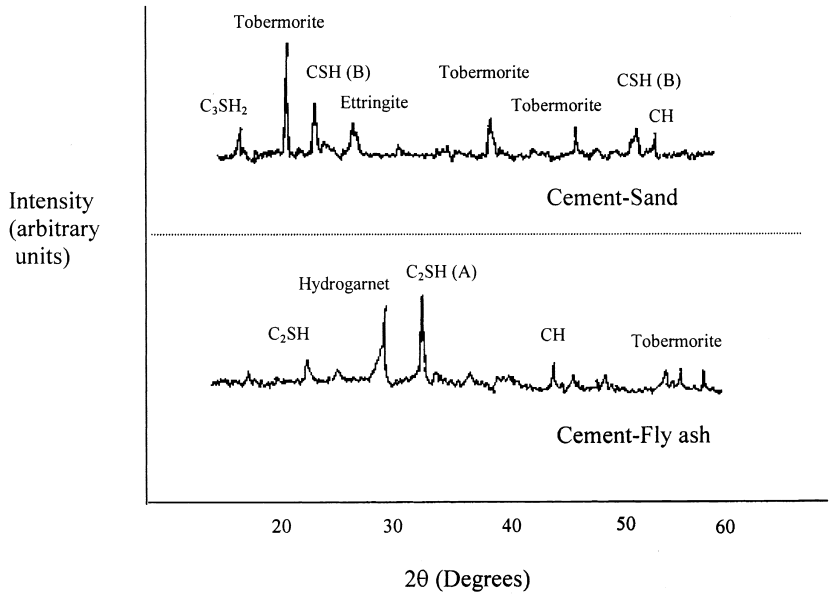

Fig. 13. XRD patterns of AAC.

cause of the relative variations in degree of hydration with time. While cement alone hydrates in the former case, the latter is characterized by fly ash hydration, which is a rather slow process.

(III) Non-autoclaved aerated concrete undergoes changes in structure with time whereas autoclaved products are practically stable.

(IV) Autoclaving results in higher strength because of the better crystallinity of the products formed. The efficiency of autoclaving is less when fly ash is present in the mix, the reaction products being poorly crystalline.

(V) Fly ash acts as nucleation sites for the formation of hydration products of cement. It also aids in capillary pore refinement. The reduction in capillary porosity is due to the combined effect of hollow shells or Hadley grains and the hydration mechanism.

(VI) There are clear indications of the existence of a transition zone at the void–paste interface, similar to that in concrete; the voids supposedly acting as aggregates of zero density.

(VII) The transition zone in aerated concrete is less porous than the one in normal concrete because of the constriction of the matrix by the voids and the unlimited space available for hydration as well as for bleed water to move about.

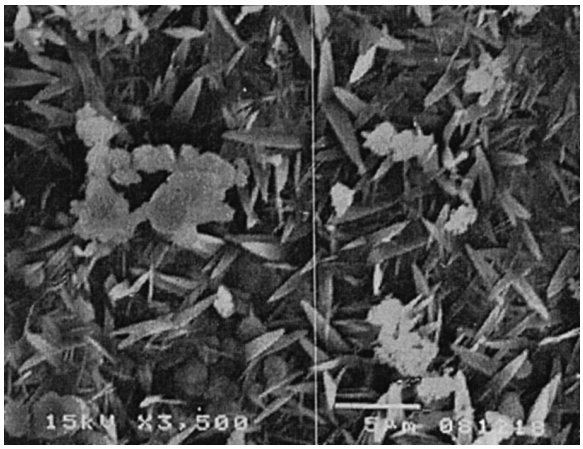

Fig. 14. Micrograph of autoclaved cement–fly ash aerated concrete (12 h).

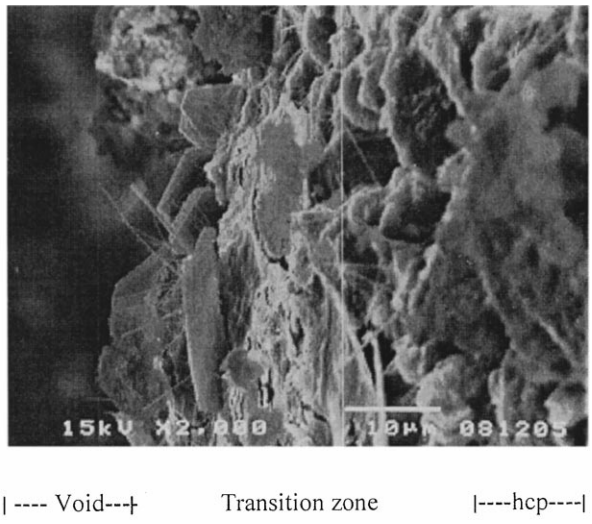

Fig. 15. Micrograph of the interfacial transition zone in aerated concrete.

References

[1] P. Prim, F.H. Witmann, Structure and water absorption of aerated concrete, in: F.H. Wittmann (Ed.), Autoclaved Aerated Concrete, Moisture and Properties, Elsevier, 1983, pp. 43–53.
[2] J. Alexanderson, Relations between structure and mechanical properties of autoclaved aerated concrete, Cem Concr Res 9 (1979) 507–514.
[3] S. Tada, S. Nakano, Microstructural approach to properties of moist cellular concrete, in: F.H. Wittmann (Ed.), Autoclaved Aerated Concrete, Moisture and Properties, Elsevier, 1983, pp. 71–89.
[4] T. Mitsuda, T. Kiribayashi, K. Sasaki, H. Ishida, Influence of hydrothermal processing on the properties of autoclaved aerated concrete, in: F.H. Wittmann (Ed.), Advances in Autoclaved Aerated Concrete, A.A. Balkema, Rotterdam, 1992, pp. 11–17.
[5] ASTM C 618 Standard specification for fly ash and raw or calcined natural pozzolan for use as a mineral admixture in portland cement concrete, American Society for Testing and Materials, Philadelphia, 1972.
[6] N. Narayanan, Influence of composition on the structure and properties of aerated concrete, MS Thesis, IIT Madras, June 1999.
[7] D.G. Montgomery, D.C. Hughes, R.I.T. Williams, Fly ash in concrete — a microstructure study, Cem Concr Res 11 (1981) 591–603.
[8] M. Frias, M.I. Sanchez de Rojas, Microstructural alterations in fly ash mortars: Study on phenomena affecting particle and pore size, Cem Concr Res 27 (1997) 619–628.
[9] K.O. Kjellsen, E.H. Atlassi, Pore structure of cement silica fume systems—presence of hollow shell pores, Cem Concr Res 29 (1999) 133–142.
[10] P.K. Mehta, P.J.M. Monteiro, Concrete-Microstructure, Properties and Materials, Indian Concrete Institute, Madras, 1997 June.
[11] S. Mindess, Tests to determine the mechanical properties of the interfacial zone, in: J.C. Maso (Ed.), Interfacial Transition Zone in Concrete, RILEM Report II, E & FN SPON, 1996, pp. 47–61.
[12] P.J.M. Monteiro, J.C. Maso, J.P. Ollivier, The aggregate–mortar interface, Cem Concr Res 15 (1985) 953–958.
[13] K.L. Scrivener, P.L. Pratt, Characterization of interfacial microstructure, in: J.C. Maso (Ed.), Interfacial Transition Zone in Concrete, RILEM Report II, E & FN SPON, 1996, pp. 3–16.
[14] R.J. Detwiler, P.J.M. Monteiro, Texture of calcium hydroxide near the cement paste–aggregate interface, Cem Concr Res 18 (1988) 823–829.
[15] A. Bentur, I. Odler, Development and nature of interfacial microstructure, in: J.C. Maso (Ed.), Interfacial Transition Zone in Concrete, RILEM Report II, E & FN SPON, 1996, pp. 18–41.
[16] M.H. Zhang, O.E. Gjorv, Microstructure of the interfacial zone between lightweight aggregate and cement paste, Cem Concr Res 20 (1990) 610–618.